TIME-FREQUENCY AND AMBIGUITY FUNCTION APPROACHES IN STRUCTURAL IDENTIFICATION

By Paolo Bonato,[1] Rosario Ceravolo,[2] and Alessandro De Stefano[3]

ABSTRACT: In the identification and control of some structures it is important to be able to resort to special techniques that may exploit environmental excitation in normal serviceability conditions. Hence, preliminary signal processing must be designed to extract significant data, even in the presence of unknown, weak, or transient excitations. In the processing and representation of nonstationary dynamic signals, great importance has been taken on in the literature by the transforms in the joint time-frequency domain. In this context, a method based on the time-frequency representation and some properties of the ambiguity function is proposed to identify the natural frequencies, draw the modal shapes, and detect nonlinearity in such testing conditions. To this end, the performances of the new Choi-Williams exponential kernel are compared with those of the Wigner-Ville transform. Finally techniques based on the instantaneous cross-correlation function are proposed to improve the performance of the identification method, and an application to a real bridge is discussed.

INTRODUCTION

The identification of a structural system represents the most important stage in any mechanical characterization process (Ghanem and Shinozuka 1995). It is generally performed in three steps

1. Formulating a reference model
2. Identifying a suitable excitation
3. Processing the measured response and determining the system parameters

Classical techniques, based on frequency response estimation, need knowledge of the input data. This leads to the use of artificial excitations, whose realization might prove very costly. Newly developed techniques have now been fine tuned to exploit the natural excitation to which a structure is subjected. Most of the methods involving unknown input data require the assumption that the environmental excitation is stationary; otherwise this gives rise to severe drawbacks in the estimate of modal parameters.

To overcome such problems, several authors have proposed the adoption of time-frequency analysis in structural identification as well as in mechanical damage assessment. Several papers have been devoted to linear time-frequency representations, namely short-time Fourier transform and wavelet transform [e.g., Staszewski and Tomlinson (1994)]. Short-time Fourier transform maps the signal into a two-dimensional function in the time-frequency plane and it is defined by assuming the signal to be stationary when it is seen through a window of limited extent. The Fourier transform of the windowed signal leads to the time-frequency distribution originally defined as a synthesis formula by Gabor (1946). An alternative view is based on a filter bank interpretation. At a given frequency, the short-time Fourier transform amounts to filtering the signal "at all times" with a band pass filter having as impulse response the window function modulated to that frequency (Rioul and Vetterli 1991).

The frequency resolution provided by this technique is limited and inversely proportional to the duration of the segment of signal transformed by applying the Fourier integral. To overcome this resolution limitation, one can imagine letting the resolution in time and frequency vary in the time-frequency plane to obtain a multiresolution analysis. This is the basic idea underlying the wavelet transform. Therefore, while the short-time Fourier transform has the same time-frequency resolution for each analysis frequency, the wavelet transform analyzes high frequencies with good time resolution but poor frequency resolution, while low frequencies are analyzed with poor time resolution but good frequency resolution.

In both cases, the squared magnitude of the linear time-frequency representation must be considered to be able to interpret the estimated distribution from an energetic point of view, thus resulting in spurious terms that result from the product among different frequency components and occur at the intersection of the transforms of each component (Kadambe and Boudreaux-Bartels 1992).

The application of bilinear transforms, such as those belonging to the Cohen class, makes it possible to overcome time-frequency resolution limitations, since these transforms are not based on signal segmentation. Particularly, Cohen class transforms are characterized by invariance to time and frequency shifts. This characteristic is very attractive when processing signals related to mechanical problems, justifying the interest recently devoted to this topic [e.g., Chiollaz and Favre (1993); Moss and Hammond (1994); De Stefano et al. (1996); Ceravolo (1996)].

However, the bilinear structure of Cohen class transforms also leads to spurious terms (called interference terms) due to cross-products between the different components constituting the signal to be processed. In failure and fault detection, such interference terms make the interpretation of the estimated distribution difficult (Wang and McFadden 1993). Different approaches to interference term filtering have been recently proposed. Each filtering approach can be considered optimal with respect to specific signal characteristics. On the contrary, when the adopted transform is not suitable with respect to the specific characteristics of the signal to be processed, the performed filtering can lead to signal distortion and, thus, loss of information. This suggests that an a priori and accurate analysis of the dynamic response of the mechanical system is of paramount importance in selecting the appropriate time-frequency transform.

In this paper we show the effectiveness of using an approach based on a time-frequency transform of the Cohen class in estimating the modal parameters of a structure. Particularly, we stress the advantage of the Choi-Williams transform (Choi and Williams 1989) over the Wigner-Ville transform, the rel-

[1]Asst. Prof., NMRC Boston Univ., 44 Cunnington St., Boston, MA 02215.

[2]Asst. Prof., Dept. of Struct. Engrg., Politecnico di Torino, c.so Duca degli Abruzzi 24, 10129 Torino, Italy.

[3]Assoc. Prof., Dept. of Struct. Engrg., Politecnico di Torino, c.so Duca degli Abruzzi 24, 10129 Torino, Italy.

Note. Associate Editor: Dimitrios Karamanlidis. Discussion open until May 1, 1998. To extend the closing date one month, a written request must be filed with the ASCE Manager of Journals. The manuscript for this paper was submitted for review and possible publication on July 29, 1996. This paper is part of the ***Journal of Engineering Mechanics***, Vol. 123, No. 12, December, 1997. ©ASCE, ISSN 0733-9399/97/0012-1260–1267/$4.00 + $.50 per page. Paper No. 13806.

J. Eng. Mech. 1997.123:1260-1267.

evance of the filtering function introduced by the kernel of the transform in the ambiguity domain (Cohen 1989), and the benefit derived by time frequency transforming cross-correlated channels recorded at different points of the studied structure.

THEORETICAL BACKGROUND

The Cohen class of transforms makes it possible to obtain time-frequency representations (TFRs) possessing the important property of being invariant to time and frequency shifts. The formula given in the following equation defines every member belonging to such class (Cohen 1989):

$$D(t,f) = \int_{-\infty}^{\infty}\int_{-\infty}^{\infty}\int_{-\infty}^{\infty} s(t' + \tau/2)s^*(t' - \tau/2)g(\theta,\tau)e^{-j2\pi\theta(t'-t)}e^{-j2\pi f\tau}\,d\theta\,dt'\,d\tau \quad (1)$$

where $s(t)$ = signal; $s^*(t)$ = its complex conjugate; t = time, f = frequency; τ = time delay; θ = frequency delay; $g(\theta, \tau)$ = kernel of the transform; and $D(t, f)$ = generic distribution belonging to the Cohen class. The correlation product $R(t, \tau) = s(t + \tau/2)\, s^*(t - \tau/2)$ is usually referred to as the instantaneous autocorrelation function. The formula adopted guarantees the instantaneous autocorrelation function to be Hermitian. Therefore, if $g(\theta, \tau) = g^*(-\theta, -\tau)$, the distribution is real-valued.

The Wigner-Ville distribution (WVD) can be obtained through (1) by setting $g(\theta, \tau) = 1$. It may be interpreted as a two-dimensional distribution of signal energy over the time-frequency plane. Besides, it satisfies the marginal properties, as expressed by the following relationships:

$$\int_{-\infty}^{+\infty} D_s(t,f)\,df = p_s(t) = |s(t)|^2 \quad (2)$$

$$\int_{-\infty}^{+\infty} D_s(t,f)\,dt = P_s(f) = |S(f)|^2 \quad (3)$$

where $|s(t)|^2$ = "instantaneous power"; and $|S(f)|^2$ = "power spectral density." Consequently, for signal energy E_S we shall find

$$E_S = \int_{-\infty}^{+\infty} |s(t)|^2\,dt = \int_{-\infty}^{+\infty} |S(f)|^2\,df = \int_{-\infty}^{+\infty}\int_{-\infty}^{+\infty} D_s(t,f)\,dt\,df \quad (4)$$

However, marginal properties do not imply that we may interpret $D_s(t, f)$ as a pointwise time-frequency energy. The WVD satisfies a large number of desirable properties (Cohen 1989). Unfortunately, it suffers from interference terms, namely, terms related to the cross-products among different frequency components caused by the bilinearity of the transform (Hlawatsch and Boudreaux-Bartels 1992).

The Choi-Williams distribution (CWD) (Choi and Williams 1989), characterized by $g(\theta, \tau) = \exp[-(\theta^2 \cdot \tau^2)/\sigma]$, also belongs to the Cohen class. It satisfies a large number of desirable properties, although a subset of those satisfied by the WVD are also satisfied by the CWD. The kernel of the transform is defined in the (θ, τ) plane, which is generally referred to as the ambiguity function plane. If the value of σ is very large, the kernel is approximately equal to 1 everywhere, thus leading to the WVD. Otherwise, the application of the kernel will have a filtering effect. In the ambiguity plane, it consists of obtaining the characteristic function, or generalized ambiguity function, by multiplying the kernel by the ambiguity function, as shown as follows:

$$M(\theta,\tau) = g_{cw}(\theta,\tau)AF(\theta,\tau)$$

where

$$AF(\theta,\tau) = \int_{-\infty}^{\infty} s(t + \tau/2)s^*(t - \tau/2)e^{-j2\pi\theta t}\,dt \quad (5)$$

Then, comparing with (1), the following statement holds:

$$D(t,f) = \int_{-\infty}^{\infty} M(\theta,\tau)e^{2\pi j\theta t}\cdot e^{-2\pi jf\tau}\cdot d\theta\cdot d\tau \quad (6)$$

$AF(\theta, \tau)$ is the "ambiguity function" of $s(t)$, and $M(\theta, \tau)$ is the "characteristic function." For small values of σ, the effect of the multiplication is to preserve the ambiguity function close to the origin of the (θ, τ) plane and to attenuate the components that are far from the axes. Since in multicomponent signals the authentic terms are generally close to the axes of the ambiguity plane while the interference terms are scattered away from them, the resulting characteristic function may suppress the interference terms without markedly affecting the signal components (Choi and Williams 1989). A more detailed discussion is provided by the following section.

The location of the signal components and the interference terms in the ambiguity plane depends on the signal characteristics. Hence, the σ value must be adapted for each specific application (Zaveri et al. 1992). We found $\sigma = 0.1 \div 1$ to be the most suitable range for structural purposes (Ceravolo 1996). Generally, if a linear identification of modal shapes and frequencies is required, a sharp filter gives good results (low σ value), while, if the system response is nonlinear and information about frequency shifts are important, a larger σ is more reliable because a sharp filter can lead to slight but not well-predictable loss in signal energy.

AUTO- AND CROSS-TFRs OF MULTICOMPONENT MECHANICAL SIGNALS

It is difficult to find a simple way to provide a definition of multicomponent signals. The most straightforward case of a multicomponent signal is the signal that has components that, when taken individually, would produce distinct contributions at particular time and frequency values (Choi and Williams 1989). When dealing with signals acquired on a structure, in the time-frequency plane, we shall distinguish, for instance, the spectral components corresponding to the energy of the individual vibration modes.

Let us assume we are working with signals acquired on a structure modeled in a discrete manner with n degrees of freedom. Let $s_i(t)$ be the displacement at the ith position, $q^{(k)}(t)$ the displacement associated with the kth vibration mode, and, finally, let $u_i^{(k)}$ be the general term of the matrix of normalized eigenvectors; then we get

$$s_i(t) = \sum_k u_i^{(k)} q^{(k)}(t) \quad (7)$$

Let us also assume that the structure, subjected to ambient excitation, is instrumented with simultaneous acquisition channels according to some of the n degrees of freedom (single setup); then the individual modal component of the ith channel can be written as

$$s_i^{(k)}(t) = u_i^{(k)} q^{(k)}(t) \quad (8)$$

In the general case of cross correlations between channels $[s_i^{(k)}(t),\ s_j^{(h)}(t)]$, the distribution will consist of autoterms and cross-terms

$$D_{s_i s_j}(t,f) = \sum_k \sum_h u_i^{(k)} u_j^{(h)} D_{q^{(k)}q^{(h)}}(t,f) = \sum_k u_i^{(k)} u_j^{(k)} D_{q^{(k)}q^{(k)}}(t,f) + \sum_{k\neq h}\sum u_i^{(k)} u_j^{(h)} D_{q^{(k)}q^{(h)}}(t,f) \quad (9)$$

where the expression

J. Eng. Mech. 1997.123:1260-1267.

$$D_{q^{(k)}q^{(h)}}(t, f) = \int_{-\infty}^{+\infty}\int_{-\infty}^{+\infty}\int_{-\infty}^{+\infty} q^{(k)}(t' + \tau/2)q^{(h)*}(t' - \tau/2)$$

$$\cdot g(\vartheta, \tau)e^{-j2\pi\vartheta(t'-t)}e^{-j2\pi f\tau}\, d\vartheta\, dt'\, d\tau \tag{10}$$

represents the generic autoterm when $k = h$ or the generic cross-term of the transform when $k \neq h$.

When we consider signals recorded on bridge structures, peaks will appear at the modal frequencies in the time-frequency representation and possibly at the typical frequencies of the traffic excitation (eigenfrequencies of the axles or the suspension systems—frequencies due to wheel-road surface interaction). In this case, we may assume that $q^{(k)}(t)$, in terms of analytic signal, is of the form

$$q^{(k)}(t) = A^{(k)}(t)e^{j[2\pi f^{(k)}t + \phi^{(k)}(t)]} \tag{11a}$$

$$q^{(h)*}(t) = A^{(h)}(t)e^{-j[2\pi f^{(h)}t + \phi^{(h)}(t)]} \tag{11b}$$

The instantaneous correlation function $[q^{(k)}(t + \tau/2)q^{(h)*}(t - \tau/2)]$ relative to the autoterms of the transform will be written as

$$R_{q^{(k)}q^{(k)*}}(t, \tau) = A^{(k)}(t + \tau/2)A^{(k)}(t - \tau/2)e^{j[2\pi f^{(k)}\tau]}e^{j[\phi^{(k)}(t+\tau/2) - \phi^{(k)}(t-\tau/2)]} \tag{12}$$

while for the cross-terms, the instantaneous correlation function will be

$$R_{q^{(k)}q^{(h)*}}(t, \tau) = A^{(k)}(t + \tau/2)A^{(h)}(t - \tau/2)e^{j[2\pi(f^{(k)}+f^{(h)})/2\cdot\tau]}$$

$$\cdot e^{j2\pi[f^{(k)}-f^{(h)}]t}e^{j[\phi^{(k)}(t+\tau/2) - \phi^{(h)}(t-\tau/2)]} \tag{13}$$

Eqs. (12) and (13) show that, in the case of amplitude and phase expressions that are not time dependent, the autoterms lead to a time-frequency representation that reports the frequencies that are common to both channels, while the cross-terms are oscillatory components that are interposed between the latter at frequencies equal to the mean frequencies of the individual cross-correlated components. The assumption of time independency of amplitude and phase has been introduced for an easier and intuitive understanding, but it is not strictly necessary. In actual fact, this is a more general outcome extending to the time-frequency representation of multicomponent signals that develop spurious terms located at the midpoint among the signal components in the time-frequency plane [see Hlawatsch and Boudreaux-Bartels (1992) for more details].

The accelerometric signals from a real bridge structure show a time-dependent amplitude. In this case, time-frequency distributions are much more powerful tools than stationary spectra for decoupling close modes, since each mode is excited with different energy in different times. In other words, a modal component can disappear in some time intervals and become dominant in some others.

In the time-frequency representation, the presence of the cross-terms may cause problems in automatic map interpretation. In the ambiguity function domain, the cross-terms are located away from the axes and therefore can be suppressed by transforms such as the CWD, which only retain the components falling in the proximity of the axes. It should be kept in mind, however, that this involves some trade-off between the attenuation of spurious components, namely the cross-terms, and the resolution of autoterm signal components.

Finally, note that by cross-correlating channels located in nodal positions [for which $u_i^{(k)} \cong 0$ for a certain number of modes k] we achieve a considerable simplification of the maps and it becomes possible to solve the problems arising from the close coupling of modal frequencies.

Interpretation in Ambiguity Function Domain

The time-frequency distribution formulated in (9) has a dual image in the ambiguity function plane. In fact, for the generic component we get

$$M_{q^{(k)}q^{(h)}}(\theta, \tau) = g_{cw}(\theta, \tau)AF_{q^{(k)}q^{(h)}}(\theta, \tau) \tag{14}$$

where

$$AF_{q^{(k)}q^{(h)}}(\theta, \tau) = \int_{-\infty}^{\infty} q^{(k)}(t + \tau/2)q^{(h)*}(t - \tau/2)e^{-j2\pi\theta t}\, dt \tag{15}$$

hence

$$M_{s_is_j}(t, f) = \sum_k u_i^{(k)}u_j^{(k)}M_{q^{(k)}q^{(k)}}(\theta, \tau) + \sum_{k\neq h}\sum u_i^{(k)}u_j^{(h)}M_{q^{(k)}q^{(h)}}(\theta, \tau) \tag{16}$$

Furthermore, if we refer to (12) and (13) and assume again, only for the sake of simplicity, the modulating factors to be replaced by a constant, we shall find

$$M_{q^{(k)}q^{(h)}}(\theta, \tau) = A^{(k)}A^{(h)}e^{j[\phi^{(k)}-\phi^{(h)}]}g(\theta, \tau)$$

$$\cdot e^{j[2\pi(f^{(k)}+f^{(h)}/2)\tau]}\delta\{\theta - [f^{(k)} - f^{(h)}]\} \tag{17}$$

where δ is the Dirac impulse.

Eq. (17) shows that, in the ambiguity function plane, the generic autoterm component falls on the τ-axis ($\theta = 0$) when $f^{(k)} = f^{(h)}$, as $\delta[\theta - [f^{(k)} - f^{(h)}]\} = \delta(\theta)$, while it falls at a distance $f^{(k)} - f^{(h)}$ from the axis when these two frequencies do not coincide. This makes it easier to understand why the choice of filtering by a kernel in the ambiguity domain that attenuates the terms apart from the axes leads to the selection of the components common to both channels.

NUMERICAL APPLICATIONS

To show the capabilities of the transforms belonging to the Cohen class in the analysis of structural dynamic response, their properties can be illustrated with the aid of simple, artificial signals.

Let us examine an application of the proposed method to the instantaneous cross-correlation of two artificial signals

$$s_a = A_1(t)\sin(2\pi f_1 t) + A_2(t)\sin(2\pi f_2 t); \quad s_b = A_1(t)\sin(2\pi f_1 t) \tag{18a,b}$$

where $f_1 = 3.2$ Hz; $f_2 = 4$ Hz; and the envelopes $A_1(t)$, $A_2(t)$ consist of square waveforms.

Fig. 1 shows the time course of the two artificial signals as well as their cross-WVD and their cross-CWD ($\sigma = 0.4$). Only two components are observed, the f_1 correlated component and an interference term in $(f_1 + f_2)/2$, which is filtered out in the CWD.

Fig. 2 shows the cross-ambiguity function of the two signals as well as the contour of the kernel of the CWD. The autoterm component stands on the τ-axis, while the interferent component is slightly apart from it. A correct choice of the σ parameter will allow the exponential CWD filtering kernel to almost totally reject such spurious components. As can be seen from this figure, only a minimal part of the spurious component is not attenuated by the kernel shape.

Let us now examine the signals originating from nonlinear SDOFs. Fig. 3 and Table 1 summarize the data of an elastic-flat nonlinear system (an ideal machine without hysteresis). Fig. 4(a) depicts the WVD of the system's oscillations with decreasing amplitude. Over the first portion, the nonlinearity is reflected in the appearance of a certain number of subject harmonics and a marked shifting of the spectral lines. The subharmonic components are physically consistent as they are connected

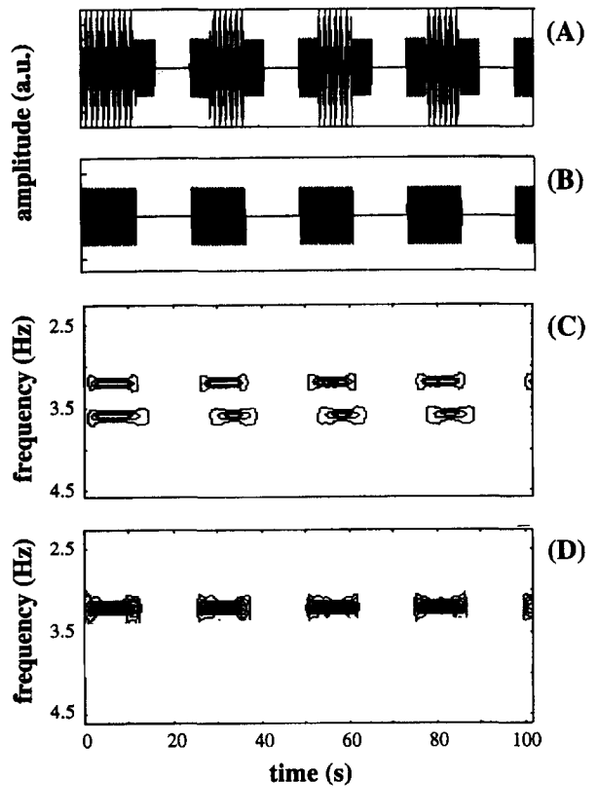

FIG. 1. (a) Plot of Time Course of Artificial Signals (Eq. 18a); (b) Plot of Time Course of Artificial Signals (Eq. 18b); (c) Cross-WVD of Signals; (d) Cross-CWD of Signals

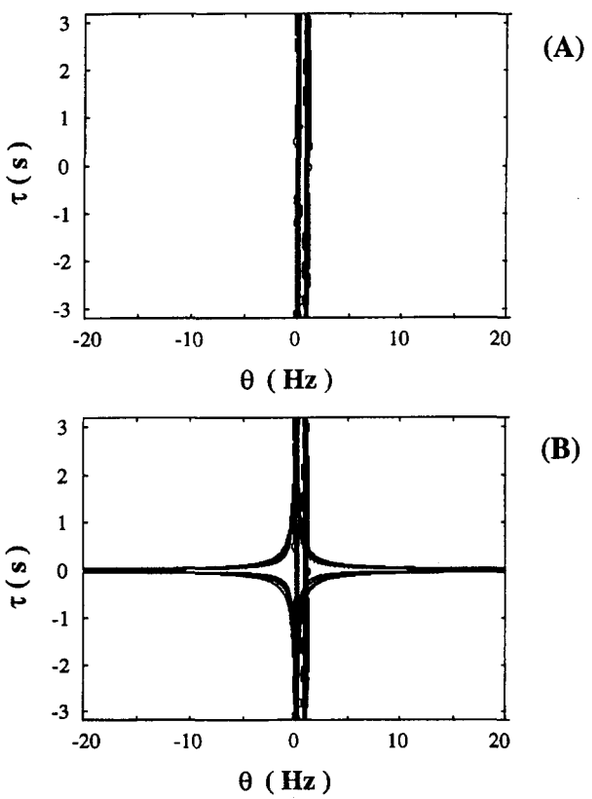

FIG. 2. (a) Contour Plot of Cross-Ambiguity Function of Signals Reported in Fig. 1; (b) Kernel of CWD Superimposed to Cross-Ambiguity Function

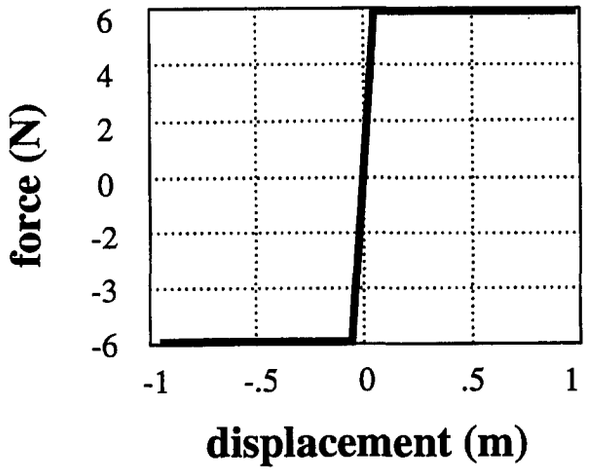

FIG. 3. Nonlinear Constitutive Law

TABLE 1. Elastoplastic Constitutive Law: Parameter Data

Parameter name (1)	Parameter value (2)
Linear stiffness	$k = 120$ N/m
Mass	$m = 1$ kg
Viscous damping	$c = 0.1$ Ns/m
Upper bound	$F_s = 6$ N
Lower bound	$F_i = -6$ N
Initial amplitude	$a = 1$ m

with each specific type of nonlinearity (Nayfeh 1973). The final portion, corresponding to linear oscillations, naturally reduces to a simple spectral line with constant frequency. Fig. 4(b) shows that the CWD only retains the consistent subharmonics. In other words, the WVD results in a multiplication of the components, engendering confusion between autoterms and spurious signal terms. This aspect offers a clear understanding of the importance of kernel filtering in the ambiguity function domain.

Application to Real Bridge Identification

The time-frequency representation makes it possible to fine tune identification methods based on preventive decoupling with the aid of modal filters. Thanks to the new representation, it is possible to devise ad hoc filters that may adapt to the nonstationary and/or nonlinear nature of the phenomenon. Filtering can also be performed directly in the time-frequency domain. In this case, we focus on "masking" the distribution (Boudreaux-Bartels and Parks 1986). At any rate, all these aspects are being investigated further through studies in the field of signal processing. Later on, we provide an example by summarizing the methodology employed in the identification of a large span bridge. The application example refers to the signals picked up on the Queensborough Bridge in Vancouver by Dr. Felberg of EDI Ltd. (Ventura et al. 1994; De Stefano et al. 1996).

The bridge, which is subjected to ambient noise, was instrumented with eight accelerometers simultaneously online during eight separate recording sessions (set ups) to collect a total of 46 sets of accelerometric data, corresponding to as many distinct positions along the longitudinal development, as shown in Fig. 5. All data were sampled at 40 Hz. The excitation caused by heavy traffic produced vertical acceleration peaks of over $0.12g$.

A CWD computation routine made it possible to analyze the data obtained on the bridge. Fig. 6 illustrates the representation of a single signal in the time-frequency domain. It

J. Eng. Mech. 1997.123:1260-1267.

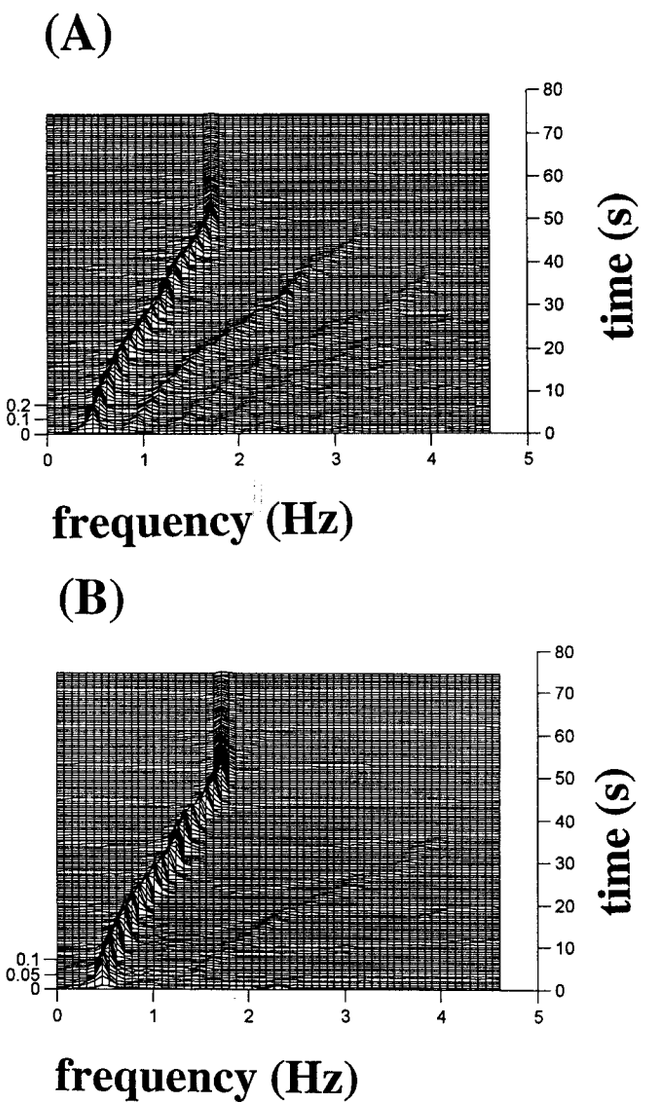

FIG. 4. Time-Frequency Representation of Free Oscillations of Elastoplastic System (Acceleration)—3D Representation: (a) WVD; (b) CWD

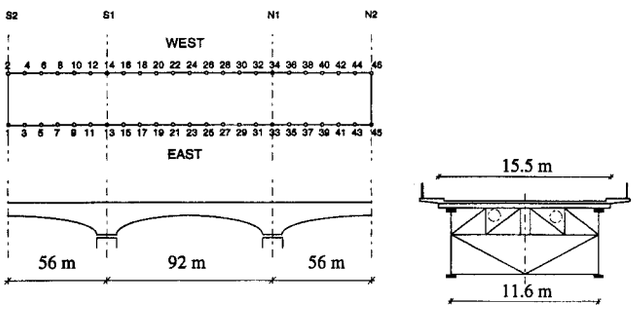

FIG. 5. Scheme of Queensborough Bridge—Measurement Points along Its Longitudinal Development and Schematic Section of Steel Girder

clearly shows the nonstationary nature of the phenomenon as a sequence of transients, which underscores the effectiveness of the proposed representation.

Selective filtering was carried out on the frequencies obtained from the observation of representations in the time-frequency domain. In particular, it was centered on the following frequencies: 1.10, 1.87, 2.28, 2.42, 3.20, and 3.45 Hz, corresponding to observable peaks in the TFRs of most measuring sessions.

Chebyshev filters (equiripple in the stop band) were used, with 0.1 Hz bandwidth, 0.1 Hz transition band, 3 dB of pass band attenuation, and 60 dB of stop band attenuation, values that actually are doubled by the noncausal IIR implementation (Oppenheim and Schafer 1975). Filters were of order higher or greater than 5.

Once filtered, the signals coming in from the different measurement points, all of them active simultaneously (single setup), were aligned by a high resolution alignment technique (McGill and Dorfman 1984) and phase data were extracted. The band pass filtered signals relating to the different channels were then rectified and subjected to a 100 coefficient FIR low-pass filter with 0.4 Hz cutoff frequency implemented by a Hanning window to extract the vibration envelopes. The maximum amplitude of each envelope was subdivided into 20 equal intervals. The envelope curves were then subdivided into 20 segments corresponding to such intervals.

After that, the mean amplitude within each interval was correlated to the mean amplitude obtained over the same time interval by the envelope of the data recorded at point 9 (see Fig. 5). This made it possible to plot curves describing the relative amplitude of modal vibration as a function of the signal's energy level. This relative amplitude was seen to be sub-

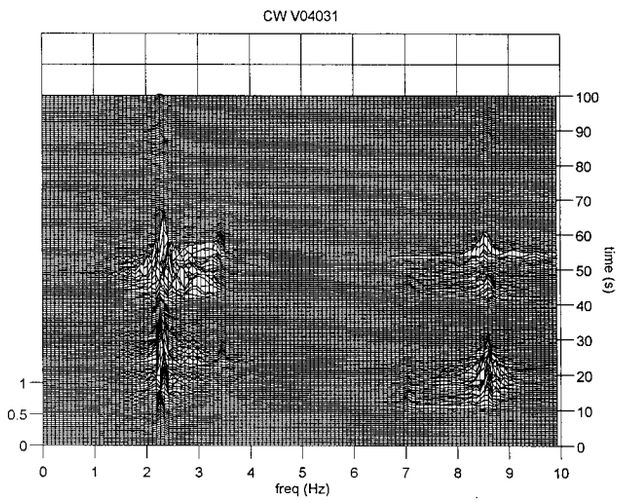

FIG. 6. CWD (σ = 0.4) of Bridge Signal Recorded at Position 7 as Reported by Fig. 5

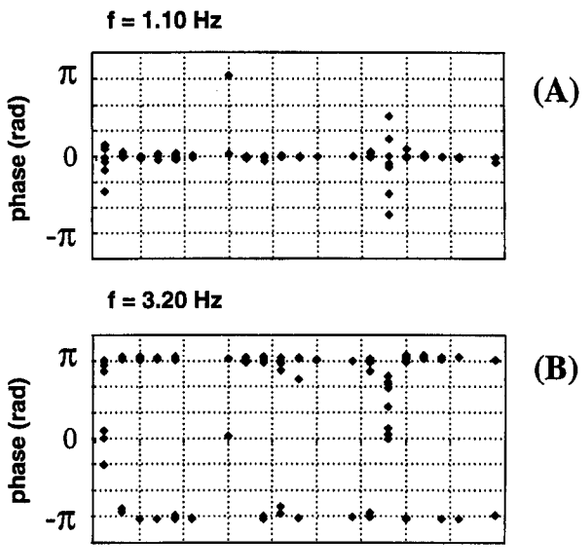

FIG. 7. Phase Estimates: (a) Relative to Flexural Modes; (b) Relative to Torsional Mode

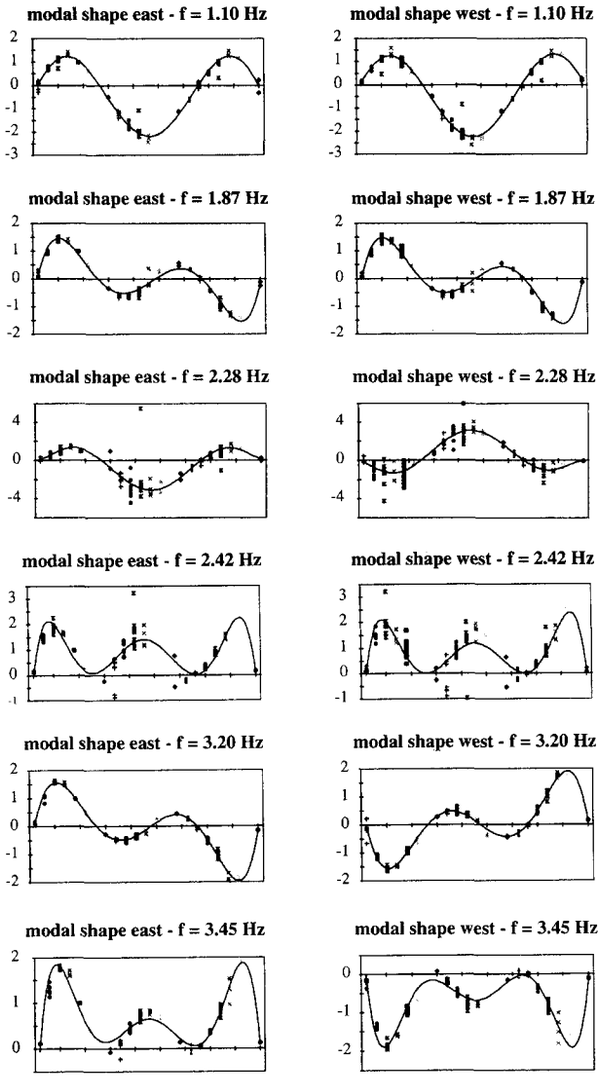

FIG. 8. First Six Modal Shapes Evaluated, Plotted by Sixth Degree Polynomial Interpolation of Points Representing Mean Values of Modal Amplitude (Different Symbols Represent Eight Different Setups)

stantially constant, provided that the energy level exceeded a certain range of values characterized by the dominance of the background noise. In other words, the procedure provided information concerning the significance threshold of the signals, estimated around 6×10^{-3} V for all examined modes.

The value of relative amplitude, as determined over the significant portion, i.e., over the significance threshold, when associated point by point to the estimated phase, which almost invariably stabilizes around 0 or π, makes it possible to plot the modal shape diagrams. Fig. 7 presents the phase estimates relative to a flexural and a torsional mode. Fig. 8 shows the complete set of the first six modal shapes evaluated, superimposed to the sixth degree polynomial interpolated function based on the mean values of local amplitude. Finally, by fitting with exponential curves the filtered signal decay after transient events, the relative damping average estimate, covering the range 0.03–0.05 for different modes, is carried out.

Comparison with Other Techniques

Let us now compare the results provided by this method with those obtained from the same data by two different research teams using different techniques (Brincker et al. 1996): the research group of the Department of Mechanics of the Politecnico di Torino (Giorcelli et al. 1996), which used autoregressive ARMAV models in the time domain; and a group working at the University of Aalborg, Denmark (Asmussen et al. 1996), which used an approach combining the random decrement domain (RDD) and the Ibrahim time domain (ITD) techniques.

As can be seen from Fig. 9 and Table 2, modal frequency estimates are almost identical for the three different approaches. The modal shape is reconstructed with comparable reliability for uncoupled modes. The time-frequency (T-STRUC) approach seems to be somehow weaker for coupled modes. The different degree of effectiveness in isolating coupled modes stems from the fact that the Aalborg and T-MEC methods use cross-correlated data from different channels, which prove more efficient to this end than the autocorrelated data adopted in the T-STRUC model. On the other hand, the time-frequency distribution has a meaningful physical readability and can reveal slight natural frequency changes due to heavy vehicle traffic.

Modal damping is always critical to detect and actual reliability is not known. The Aalborg approach uses a full time sample to calculate the data correlations. Slight nonstationarity, e.g., due to transient mass additions, could cause slow changes in correlation function amplitudes similar to the effect of higher damping. Such effects, however, depend on the maximum time delay in correlation functions.

The T-MEC approach leads to the damping coefficient estimates based on the complex nature of the eigenvalues. Damping could be evaluated more efficiently because the ARMAV algorithm is applied in short-time windows, affording a better protection against nonstationarity, but this is accom-

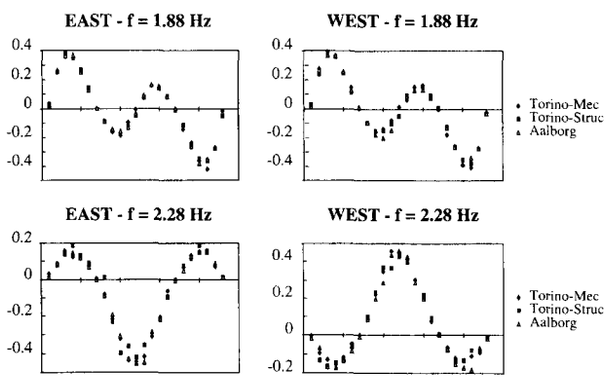

FIG. 9. Comparison of Estimates of Modal Shapes Obtained by Three Different Approaches

TABLE 2. Compared Estimates of Modal Parameters

Mode (1)	Frequency (Hz) T-MEC (2)	T-STRUC (3)	Aalborg (4)	Damping (%) T-MEC (5)	T-STRUC (6)	Aalborg (7)
1 Flexural	1.12	1.10	1.10	1.94	5	7.36
2 Flexural	1.88	1.87	1.88	0.87	3.1	1.45
3 Torsional	2.29	2.28	2.28	0.49	—	1.86
4 Flexural	2.42	2.42	2.42	0.84	—	2.15
5 Torsional	3.20	3.20	3.20	0.78	—	1.51
6 Torsional	3.43	3.45	3.44	0.58	—	1.08
7 Flexural	3.70	3.74	3.73	1.4	—	1.68
8 Torsional	5.15	5.16	5.15	0.25	—	0.64
9 Flexural	5.78	5.84	5.74	0.96	—	1.15
10 Torsional	7.04	7.12	7.01	0.65	—	0.77
11 Torsional	7.52	7.52	7.53	0.82	—	0.69
12 Torsional	8.56	8.64	—	0.32	—	—

Note: T-MEC = Dept. of Mechanics, Politecnico di Torino, Turin, Italy; T-STRUCT = Dept. of Structural Engineering, Politecnico di Torino, Turin, Italy; Aalborg = Dept. of Build. Technol. and Struct. Engrg., Aalborg University, Aalborg, Denmark.

J. Eng. Mech. 1997.123:1260-1267.

plished only if the sampling ratio is well chosen and the signal-to-noise ratio is good enough.

The T-STRUC model makes it possible to evaluate the damping factor through the free decay of filtered time histories after transient loading. This method, unlike the previous two, does not make any hypothesis about the stationarity of structural response, but a correct evaluation requires some experimental records in conditions of low traffic to be sure that the decay after a transient event is free from disturbances.

Effectiveness of Instantaneous Cross-Correlation in Decoupling Modes

To extend the demonstration of the properties of the instantaneous cross-correlation function, two channels of a single setup were analyzed (position 7 and position 23, see Fig. 5), the second channel being close to a fifth mode node. The two signals, previously filtered in the 3–3.6 Hz range, were first autocorrelated separately, by means of a Choi-Williams transform ($\sigma = 0.1$)—Fig. 10(a) shows the coupling of the modes on the recording performed at position 7, while Fig. 10(b) confirms that on the recording performed at position 23, the energy of the fifth mode is very weak (nodal position).

Figs. 10(c) and 10(d) show the cross-CWD with σ equal to 0.1 and 0.01, respectively. These plots outline the removal of energy on the component that was not present on both channels, as well as the attenuation of spurious terms.

Fig. 11 shows the simplification of the map accomplished by the CWD focusing on a time interval shorter than that reported by the previous figure. This result is of paramount importance in the presence of several coupled modes and may be valuable in connection with the use of automatic pattern recognition procedures.

Hence, the instantaneous cross-correlation between appropriate channels can filter unknown and nonstationary components through the application of a filtering function in the cross-ambiguity domain. Therefore it can decouple components, which are correlated in frequency but uncorrelated in time (coupled modes).

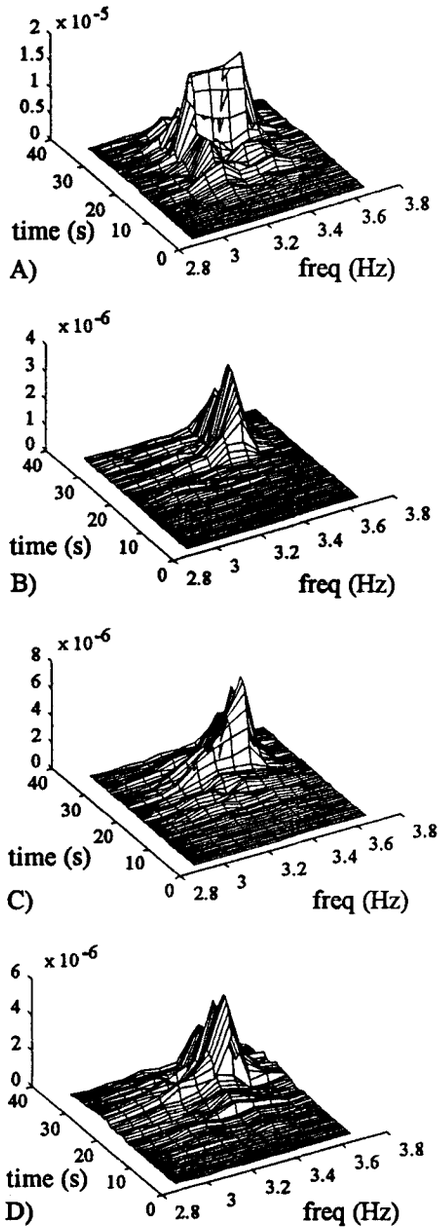

FIG. 10. 3D Representations of CWDs of Bridge Signals: (a) CWD of Signal Recorded at Position 7; (b) CWD of Signal Recorded at Position 23; (c) Cross-CWD ($\sigma = 0.1$) of Signals Recorded at Positions 7 and 23; (d) Cross-CWD ($\sigma = 0.01$) of Signals Recorded at Positions 7 and 23

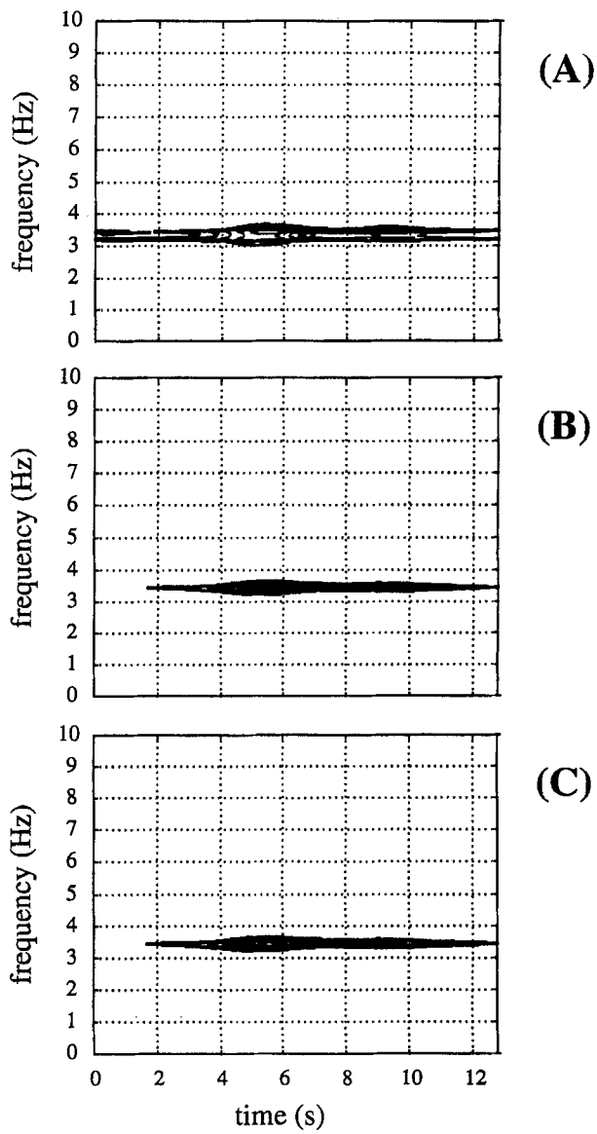

FIG. 11. Contour Plots of CWDs of Bridge Signals: (a) CWD of Signal Recorded at Position 7; (b) CWD of Signal Recorded at Position 23; (c) Cross-CWD ($\sigma = 0.1$) of Signals Recorded at Positions 7 and 23

CONCLUSIONS

Theoretical and application results confirm the effectiveness of the time-frequency representation in the analysis of nonstationary signals and the identification of structures in serviceability conditions.

In the field of defect detection, these tools are already employed in conjunction with pattern recognition techniques, but they also appear to be promising in the field of nonlinearity detection, since nonlinearity leads to deviations of spectral lines in the transient intervals.

Finally, the use of instantaneous cross-correlation may improve map quality for purposes of automatic interpretation processes, and furthermore, it may provide solutions to some of the problems associated with close coupling of modes.

Further investigations will focus on improved filtering in the ambiguity function domain and also will be resorting to masking techniques. The effects of such filters will be calibrated by means of suitable test data.

APPENDIX I. REFERENCES

Asmussen, J. C., Ibrahim, S. R., and Brincker, R. (1996). "Random decrement and regression analysis of traffic responses of bridges." *Proc., 14th Int. Modal Anal. Conf.*, 453–458.

Boudreaux-Bartels, G. F., and Parks, T. W. (1986). "Time-varying filtering and signal estimation using Wigner distribution synthesis techniques." *IEEE Trans., Acoustics, Speech, Signal Processing*, 34, 442–451.

Brincker, R., De Stefano, A., and Piombo, B. (1996). "Ambient data to analyse the dynamic behaviour of bridges: A first comparison between different techniques." *Proc., 14th Int. Modal Anal. Conf.*, 477–482.

Ceravolo, R. (1996). "Metodi Dinamici Avanzati in Diagnostica Strutturale," PhD thesis, Dept. of Struct. Engrg., Politecnico di Torino, Italy (in Italian).

Chiollaz, M., and Favre, B. (1993). "Engine noise characterisation with Wigner-Ville time-frequency analysis." *Mech. Sys. and Signal Processing*, 7, 375–400.

Choi, H. I., and Williams, W. J. (1989). "Improved time-frequency representation of multicomponent signals using exponential kernels." *IEEE Trans., Acoustics, Speech, Signal Processing*, 37, 862–871.

Cohen, L. (1989). "Time-frequency distribution: A review." *Proc. IEEE*, 77, 941–981.

De Stefano, A., Ceravolo, R., Bonato, P., Gagliati, G., and Knaflitz, M. (1996). "Analysis of ambient vibration data from Queensborough Bridge using Cohen class time-frequency distributions." *Proc., 14th Int. Modal Anal. Conf.*, 470–476.

Gabor, D. (1946). "Theory of communication." *Proc. IEEE*, 93, 429–457.

Ghanem, R., and Shinozuka, M. (1995). "Structural-system identification: Theory." *J. Engrg. Mech.*, ASCE, 121, 255–264.

Giorcelli, E., Garibaldi, L., Riva, A., and Fasana, A. (1996). "ARMAV analysis of Queensborough ambient data." *Proc., 14th Int. Modal Anal. Conf.*, 466–469.

Hlawatsch, F., and Boudreaux-Bartels, G. F. (1992). "Linear and quadratic time-frequency signal representations." *IEEE Signal Processing Mag.*, 21–67.

Kadambe, S., and Boudreaux-Bartels, G. F. (1992). "A comparison of the existence of cross-terms in the Wigner distribution and the squared magnitude of the wavelet transform and the short-time Fourier transform." *IEEE Trans. on Signal Processing*, 40, 2498–2517.

McGill, K. C., and Dorfman, L. J. (1984). "High-resolution alignment of sampled waveforms." *IEEE Trans. on Biomedical Engrg.*, 31, 462–468.

Moss, J. C., and Hammond, J. K. (1994). "A comparison between the modified spectrogram and the pseudo-Wigner-Ville distribution with and without modification." *Mech. Sys. and Signal Processing*, 8, 243–258.

Nayfeh, A. H. (1973). *Perturbation methods*. John Wiley & Sons, Inc., New York, N.Y.

Oppenheim, A. V., and Schafer, R. D. (1973). *Digital signal processing*. Prentice-Hall International, London, U.K.

Rioul, O., and Vetterli, M. (1991). "Wavelets and signal processing." *IEEE Signal Processing Mag.*, 14–38.

Staszewski, W. J., and Tomlinson, G. R. (1994). "Application of the wavelet transform to fault detection in a spur gear." *Mech. Sys. and Signal Processing*, 8, 289–307.

Ventura, C. E., Felber, A. J., and Prion, H. (1994). "Seismic evaluation of a long span bridge by modal testing." *Proc., 12th Int. Modal Anal. Conf.*, 1309–1315.

Wang, W. J., and McFadden, P. D. (1993). "Early detection of gear failure by vibration analysis. II: Interpretation of the time-frequency distribution using image processing techniques." *Mech. Sys. and Signal Processing*, 7, 205–215.

Zaveri, H. P., Williams, W. J., Iasemidis, L. D., and Sackellares, J. C. (1992). "Time-frequency representation of electrocorticograms in temporal lobe epilepsy." *IEEE Trans. on Biomedical Engrg.*, 39, 502–509.

APPENDIX II. NOTATION

The following symbols are used in this paper:

$A^{(k)}(t)$ = modal envelope;
$AF(\theta, \tau)$ = ambiguity function;
$D(t, f)$ = distribution of Cohen class;
E_S = signal energy;
f = frequency;
$f^{(k)}, f^{(h)}$ = modal frequencies;
$M(\theta, \tau)$ = generalized ambiguity function;
$q^{(k)}(t)$ = displacement of kth mode;
$R(t, \tau)$ = instantaneous autocorrelation function;
$S(f)$ = Fourier transform of $s(t)$;
$s(t)$ = generic signal;
$s_i(t)$ = displacement at ith position;
$s_i^{(k)}(t)$ = signal modal component;
t = time;
t' = time dummy variable;
δ = Dirac impulse;
θ = frequency lag;
σ = selectivity parameter; and
τ = time lag.

J. Eng. Mech. 1997.123:1260-1267.